

SYNTHESIS OF AN EFFICIENT PHOTOCATALYST (ACTIVATED CARBON SUPPORTED ZnS) FOR METHYLENE BLUE DEGRADATION

C. ZÖRER^a, O. BAYTAR^b, Ö. ŞAHİN^b, S. HOROZ^c, M. S. IZGI^{b,*}

^a*Institute of Science and Technology, Siirt University, 56100 Siirt, Turkey*

^b*Department of Chemical Engineering, Faculty of Engineering, Siirt University, 56100 Siirt, Turkey*

^c*Department of Electrical & Electronics Engineering, Faculty of Engineering, Siirt University, Siirt, Turkey*

In the present study, activated carbon (AC) supported ZnS catalysts at different concentrations of AC were synthesized using hydrothermal method. The MB photocatalytic degradation efficiency of AC supported ZnS catalysts at different concentrations of AC was examined in the presence of UV-C lamp. As a result of photocatalytic measurements, the catalyst having the best photocatalytic activation was determined. The effect of different parameters, such as the amount of catalyst and dye concentration, on the photocatalytic degradation of methylene blue was investigated in the presence of this catalyst. Moreover, The photocatalytic degradation kinetics of methylene blue in the presence of catalyst were investigated by first and second order kinetic model. In the last part of the study, structural, morphological and elemental properties of the catalyst having the best photocatalytic activity were examined by x-ray diffraction (XRD), scanning electron microscope (SEM) and energy dispersive x-ray (EDX) measurements, respectively.

(Received February 19, 2020; Accepted July 7, 2020)

Keywords: Activated carbon, Characterization, Photocatalytic, Synthesis, ZnS

1. Introduction

Semiconductors and metal nanoparticles are among the focal points of scientific research in recent years. Particle sizes were found to be very important in determining the properties of these materials [1, 2]. Due to their unique electronic nature, they have many potential applications, such as energy conversion systems [3], biological labels [4], electroluminescence devices [5], quantum-dot lasers [6], and solar cells [7-12]. ZnS nanoparticles from the II-VI semiconductor group have a band gap of 3.54-3.91 eV at room temperature [13]. ZnS nanostructures are one of the most promising materials for application in different optoelectronics and photovoltaic devices, such as bio-labeling [14], transistors [15] for electronic switches, photoconductor sensors [16]. In the production of ZnS nanocrystals, hydrothermal [17], chemical precipitation [18] and sol-gel methods [19] are frequently used in the production of materials in different morphologies. Among these methods, the method of hydrothermal is preferred because it is a low cost and practical method.

Toxic and organic pollutants which are released to water and environment negatively affect human health [20]. Industrial and synthetic textile dyes constitute the most important chemical part of these pollutants. It is of great importance that these materials which are highly toxic and carcinogenic are transformed into degradable inorganic compounds [21-28]. By using catalysts such as ZnS [29], TiO₂ [30], ZnO [31], CeO₂ [32], Fe₂O₃ [33], ZrO₂ [34], and SrO₂ [35], this kind of pollutants can be removed by photocatalytic oxidation.

Methylene Blue (MB) belongs to cationic category and most toxic dye [36]. MB (thiazine (cationic) dye) commonly used for coloring paper, temporary hair colorant, dyeing cottons, wools

* Corresponding author: saitizgi@siirt.edu.tr

and so on [37]. MB lead to health hazards such as difficulties in breathing, vomiting, diarrhea, and nausea [38]. Therefore, its removal and elimination from various aqueous wastes is a requirement.

In the present study, activated carbon (AC) supported ZnS catalysts at different concentrations of AC were synthesized using hydrothermal method. The MB photocatalytic degradation efficiency of AC supported ZnS catalysts at different concentrations of AC was examined in the presence of UV-C lamp.

2. Experimental details

Activated carbon (AC) supported ZnS nanoparticles were synthesized at different AC concentrations using hydrothermal method. 2.19 g of zinc acetate and 0.61 g of thiourea in 80 ml of di-ionized water were also stirred for 30 minutes. 2.6 ml of ethylenediamine was then added to the CdS mixture. Different concentrations of AC (0%, 5%, 10% and 20%) were added to the existing mixture to synthesize ZnS nanoparticles with different concentrations of AC. The obtained mixture was vigorously stirred for 2 h and then transferred in Teflon coated stainless steel autoclave and kept at 180°C for 12 h. After completion of reaction, autoclave was cooled to room temperature. The obtained white colored powder was dried in vacuum at 70°C followed by fine crushing and labeling. The codes of prepared photocatalysts are displayed in Table 1.

Table 1. Sample names and their codes.

Sample name	Sample code
0% wt AC_ZnS	0 AC_ZnS
5% wt AC_ZnS	5 AC_ZnS
10% wt AC_ZnS	10 AC_ZnS
20% wt AC_ZnS	20 AC_ZnS

The synthesized catalysts were characterized by x-ray diffraction (XRD), scanning electron microscope (SEM) and energy dispersive x-ray (EDX) devices. The photocatalytic degradation of MB in the batch system using ZnS nanoparticles with AC was investigated in the presence of UV-C lamp. The parameters used for photocatalytic degradation tests of MB were 22 ml of solution, 25 mg of catalyst, 20 ppm of dye concentration, respectively. The concentration of MB remaining in solution was determined by UV spectroscopy. The effect of different parameters such as AC/ZnS ratio, initial concentration of dye and catalyst amount were investigated in photocatalytic degradation of MB.

3. Results and discussion

3.1. Photocatalytic activity

Photocatalytic degradation experiments of MB were performed to determine the best activated carbon/ZnS ratio. The parameters used in the experiments performed were solution volume (22 ml), dye concentration (20 ppm) and amount (25 mg) of ZnS nanoparticles with different concentrations of AC, respectively. The percentages of photocatalytic degradation obtained in the presence of different AC/ZnS ratios are shown in Fig. 1.

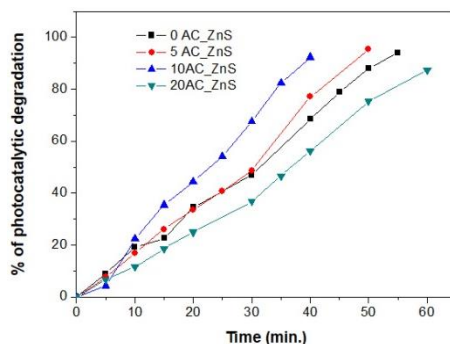


Fig. 1. The percentages of photocatalytic degradation obtained in the presence of different AC/ZnS ratios.

When AC/ZnS ratio increases from 5% to 10%. It was observed that catalyst activity increased then decreased. This is likely due to the fact that ZnS does not have sufficient activity at low AC/ZnS ratios. In addition, at high AC/ZnS ratios, ZnS overlaps and it is predicted that this reduces activity. Thus, the most effective AC/ZnS ratio was determined as 10%. This ratio was used in subsequent experiments.

One of the most important parameters in photocatalytic studies is the amount of catalyst. After determining the most effective AC/ZnS ratio was 10%, degradation experiments of MB were performed in the presence of different catalyst (10 AC_ZnS) amounts. The parameters used in the experiments performed were solution volume (22 ml), dye concentration (20 ppm) and different catalyst (10 AC_ZnS) amounts (10, 25 and 50 mg). The percentages of photocatalytic degradation obtained in the presence of different catalyst (10 AC_ZnS) amounts are indicated in Fig. 2.

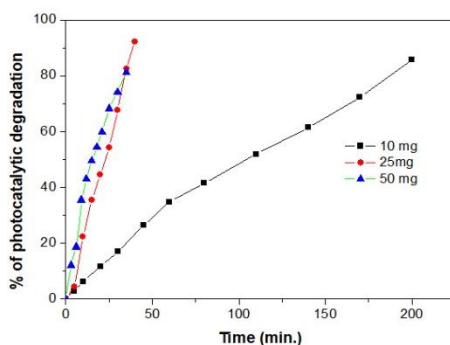


Fig. 2. The percentages of photocatalytic degradation obtained in the presence of different catalyst (10 AC_ZnS) amounts.

As shown in Fig. 2, the percentage degradation increases with increasing catalyst (10 AC_ZnS) amount from 10 mg to 50 mg. This is likely due to an increase in the amount of catalyst (10 AC_ZnS) increases the active site. Thus, the degradation activity of MB will also increase because of light adsorption on the catalyst (10 AC_ZnS) surface and the formation of OH⁻ radicals.

Dye concentration is an important parameter influencing photocatalytic studies. The parameters used in the experiments performed were solution volume (22 ml), catalyst (10 AC_ZnS) amount (25 mg) and different dye concentrations (20, 50 and 100 ppm) and. The percentages of photocatalytic degradation obtained in the presence of different dye concentrations are signalized in Fig. 3.

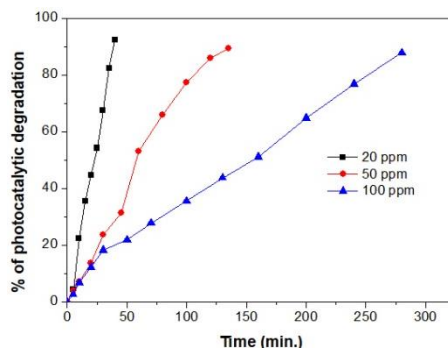


Fig. 3. The percentages of photocatalytic degradation obtained in the presence of different dye concentrations.

It is clear from the graph that percent degradation decreases with increasing concentration of MB. For example, it was observed that when the initial concentration of the solution was 20 ppm, the reaction was completed in 40 minutes, while increasing the concentration to 100 ppm, the same reaction was ended in 280 minutes. It is known that increased MB concentration increases the adsorption capacity on the catalyst surface. Therefore, the OH⁻ formed on the catalyst surface inhibits adsorption and causes a decrease in photocatalytic activation. As a result, the decrease in OH⁻ formation leads to a decrease in dye removal efficiency. Another reason for this is that based on Lambert - Beer Law, when photon entry into the solution decreases with increasing initial dye concentration, less photon adsorption occurs on the catalyst surface. As a result, this reduces the reaction rate.

The photocatalytic degradation kinetics of methylene blue in the presence of catalyst (10 AC_ZnS) were investigated by first and second order kinetic model. First and second order kinetic model equations are given below, respectively.

$$-\ln\left(\frac{C_t}{C_o}\right) = k_1 \cdot t \quad (1)$$

$$\frac{1}{C_t} - \frac{1}{C_o} = k_2 \cdot t \quad (2)$$

C_t : solution concentration at time t (mg/l), C_o : initial solution concentration at time t (mg/l), k_1 : First order adsorption rate constant (min^{-1}), k_2 : Second order adsorption rate constant (min^{-1}) and t : adsorption time (min.). The graphs obtained from the above equations are demonstrated in Fig. 4 (a-b), respectively. As can be seen from Fig. 4 (a-b), the kinetics of photocatalytic degradation of MB in the presence of catalyst (10 AC_ZnS) is first order. This result means that the photocatalytic degradation of MB is time controlled.

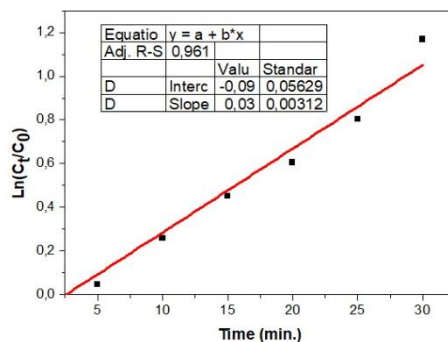


Fig. 4. (a) First order kinetic model for the photocatalytic degradation kinetics of MB in the presence of catalyst (10 AC_ZnS).

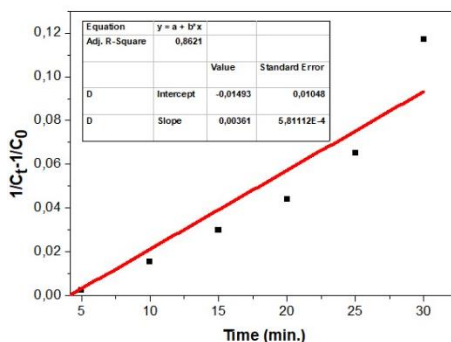


Fig. 4. (b) Second order kinetic model for the photocatalytic degradation kinetics of MB in the presence of catalyst (10 AC_ZnS).

3.2. Characterization of catalyst (10 AC_ZnS)

X-ray diffraction (XRD) technique was used to have knowledge about the crystallinity and phase structure of the catalyst (10 AC_ZnS). The XRD patterns recorded for the catalyst (10 AC_ZnS) having the most effective photocatalytic activity are pointed to in Fig. 5.

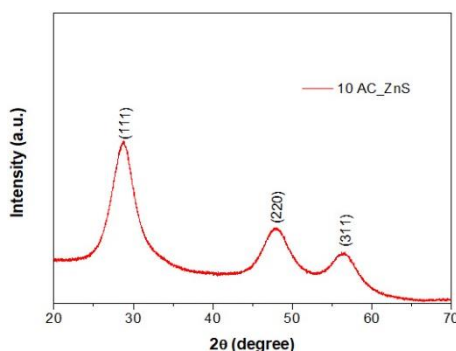


Fig. 5. The XRD patterns recorded for the catalyst (10 AC_ZnS).

The three broad diffraction patterns indicated in the Figure 5 correspond to planes (111), (220) and (311), respectively. This expresses that the synthesized catalyst (10 AC_ZnS) has a cubic structure. The result is consistent with the standard JCPDS file (JCPDS-75-1546) of ZnS. Further, the crystallite size of the catalyst (10 AC_ZnS) was calculated to be approximately 3 nm using the Scherer formula (Equation 3) given below.

$$d = \frac{0,9 \cdot \lambda}{\beta \cdot \cos \theta} \quad (3)$$

where d is the crystallite size of the catalyst (10 AC_ZnS), λ : wavelength of the XRD device, β : full width at half height in radians (FWHM) and θ : Bragg's diffraction angle.

The recorded SEM image of the AC sample is shown in Fig. 6.

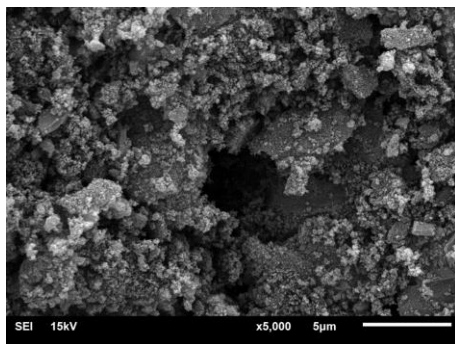


Fig. 6. The recorded a SEM image of the AC sample.

As can be clearly seen from the Fig. 6, while the presence of significant porosity was not observed on the surfaces of the AC sample, the presence of the pores was determined when the internal structures were examined. The recorded SEM image demonstrates the presence of meso and micropores rather than macro pores.

Fig. 7 indicates the recorded SEM image of the catalyst (10 AC_ZnS). As the image infers, the catalyst (10 AC_ZnS) was formed in the form of pellets. It has been observed that these lumps come together to form clumps on the surface. It was also observed that the synthesized catalyst (10 AC_ZnS) was of different sizes due to the clumps formed. In other words, particles of different sizes can be detected within the same clump.

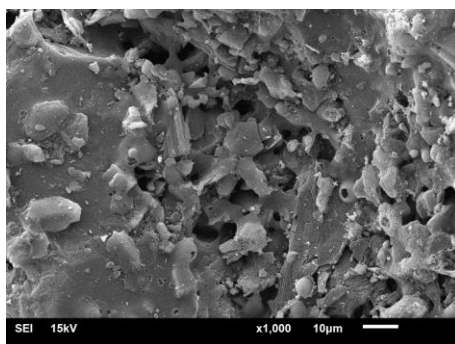


Fig. 7. The recorded a SEM image of the catalyst (10 AC_ZnS).

The EDX spectra of the AC and catalyst (10 AC_ZnS) are signalized in Fig. 8 (a-b), respectively. The observation of the desired elements in its own category, which can be clearly seen from the EDX spectra, is an indication that each sample is successfully synthesized.

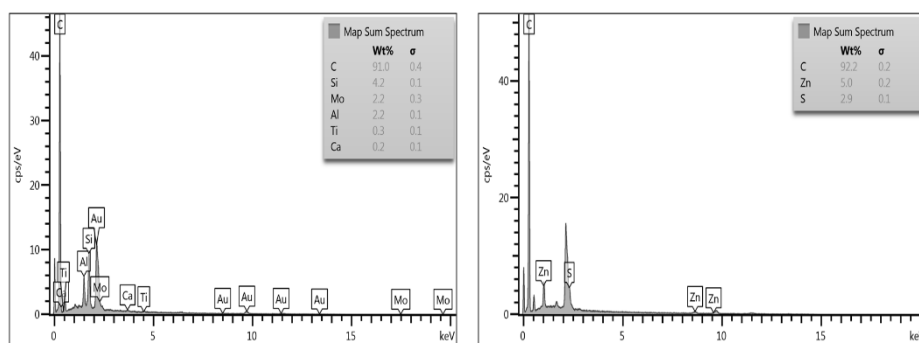


Fig. 8. EDX spectra of a) AC sample, b) catalyst (10 AC_ZnS).

4. Conclusions

In the present study, activated carbon (AC) supported ZnS catalysts at different concentrations of AC were synthesized using hydrothermal method. The MB photocatalytic degradation efficiency of AC supported ZnS catalysts at different concentrations of AC was examined in the presence of UV-C lamp. The 10 wt % of AC was determined as the ideal mass ratio for the highest photocatalytic activity. We think that our present study, using AC as a support should serve as an important approach in the field of materials sciences.

Acknowledgements

This study was supported by Research Fund of the Siirt University. Project Code: 2019 SIUFEB 05.

References

- [1] S. Horoz et al., *Journal of Materials Science: Materials in Electronics* **29**(2), 1004 (2018).
- [2] I. Khan, K. Saeed, I. Khan, *Arabian Journal of Chemistry*, 2017.
- [3] M. Wang, et al., *Advanced Science* **3**(6), 1600024 (2016).
- [4] D. M. Willard, *Analytical and Bioanalytical Chemistry* **376**(3), 284 (2003).
- [5] B. P. Chandra, V.K. Chandra, P. Jha, *Solid State Phenomena* **222**, 1 (2015).
- [6] I. Samuel, *Nature Materials* **17**, 9 (2017).
- [7] S. Horoz, *Physical Review Applied* **3**(2), 024011 (2015).
- [8] O. Baytar et al., *Journal of Materials Science: Materials in Electronics* **29**(6), 4564 (2018).
- [9] S. Horoz, *Superlattices and Microstructures* **111**, 1043 (2017).
- [10] S. Horoz, A. Ekinici, O. Sahin, *Journal of Materials Science: Materials in Electronics* **29**(7), 5830 (2018).
- [11] A. Pimachev et al., *Solid State Communications* **257**, 47 (2017).
- [12] O. Sahin, S. Horoz, *Journal of Materials Science: Materials in Electronics* **29**(19), 16775 (2018)
- [13] C. Sabitha et al., *Optical and Quantum Electronics* **50**, 2018.
- [14] S. Baruah et al., *Journal of Fluorescence* **22**, 403 (2012).
- [15] X. Wang et al., *Critical Reviews in Solid State and Materials Sciences* **38**(1), 57 (2013).
- [16] L. Hu et al., *Advanced Materials* **24**(17), 2305 (2012).
- [17] V. Sabaghi, F. Davar, Z. Fereshteh, *Ceramics International* **44**(7), 7545 (2018).
- [18] P. L. Reddy et al., *Journal of Materials Science: Materials in Electronics* **30**(5), 4676 (2019).
- [19] M. Nikzad, M. R. Khanlary, S. Rafiee, *Applied Physics A* **125**(8), 507 (2019).
- [20] S. M. Rhind, *Philosophical transactions of the Royal Society of London, Series B, Biological sciences* **364**(1534), 3391 (2009).
- [21] S. Sarkar et al., *Water Conservation Science and Engineering* **2**(4), 121 (2017).
- [22] V. Dutta et al., *Journal of Environmental Chemical Engineering* **7**(3), 103132 (2019).
- [23] D. Jamwal et al., *The Journal of Physical Chemistry C* **119**(9), 5062 (2015).
- [24] P. Raizada et al., *Journal of Photochemistry and Photobiology A: Chemistry* **374**, 22 (2019).
- [25] P. Raizada et al., *Separation and Purification Technology* **212**, 887 (2019).
- [26] P. Shandilya et al., *Journal of the Taiwan Institute of Chemical Engineers* **93**, 528 (2018).
- [27] P. Shandilya et al., *Journal of Cleaner Production* **203**, 2018.
- [28] P. Shandilya et al., *Separation and Purification Technology* **210**, 804 (2019).
- [29] H. Chen et al., *Powder Technology* **298**, 1 (2016).
- [30] Y. Choi, *Environmental Science & Technology* **51**(7), 3973 (2017).
- [31] K. M. Lee, C. W. Lai, J. C. Juan, *Corrosion Engineering, Science and Technology* **53**(7), 462 (2018).
- [32] Y. Xiao et al., *Integrated Ferroelectrics* **191**(1), 169 (2018).

- [33] M. D. Shete, J. B. Fernandes, *Bulletin of Materials Science* **42**(5), 254 (2019).
- [34] T. Sun et al., *Applied Surface Science* **416**, 656 (2017).
- [35] A. Divya et al., *AIP Conference Proceedings* **1731**(1), 140024 (2016).
- [36] M. Ghaedi et al., *Environmental Progress & Sustainable Energy* **32**(3), 535 (2013).
- [37] H. Patel, R. Vashi, *Journal of Environmental Engineering and Landscape Management* **21**, 36 (2013).
- [38] P. R. Ginimuge, S. D. Jyothi, *Journal of anaesthesiology, clinical pharmacology* **26**(4), 517 (2010).